Modeling the response of the induced magnetosphere of Venus to changing IMF direction using MESSENGER and Venus Express observations

Mehdi Benna,[1] Mario H. Acuña,[1] Brian J. Anderson,[2] Stanislav Barabash,[3] Scott A. Boardsen,[4] George Gloeckler,[5] Robert E. Gold,[2] George C. Ho,[2] Haje Korth,[2] Stamatios M. Krimigis,[2] Ralph L. McNutt Jr.,[2] Jim M. Raines,[5] Menelaos Sarantos,[4] James A. Slavin,[6] Sean C. Solomon,[6] Tielong L. Zhang,[7] and Thomas H. Zurbuchen[5]

Received 18 November 2008; revised 23 January 2009; accepted 27 January 2009; published 28 February 2009.

[1] The second MESSENGER flyby of Venus on 5 June 2007 provided a new opportunity to study the response of the induced magnetosphere of the planet to changes in the direction of the interplanetary magnetic field (IMF). At the time of the MESSENGER flyby, the European Space Agency's Venus Express spacecraft was located outside the magnetosphere and provided a monitor of solar wind conditions. Measurements by the Venus Express magnetometer show that the IMF underwent four major changes in direction and magnitude while MESSENGER was traveling through the inner magnetosphere of Venus. The response of the magnetosphere to each of these IMF changes was determined with a semi-time-dependant global magnetohydrodynamic (MHD) model, and the results were compared with magnetic and compositional measurements by the Magnetometer (MAG) and the Energetic Particle and Plasma Spectrometer (EPPS) on MESSENGER. Our modeling results show that this semi-time-dependant MHD technique produces magnetic field profiles that can account for both of the field reversals seen by MAG and the peak in the pick-up ion density measured by EPPS. Moreover, these results reveal that the plasma sheet that confines most of the pick-up ions has a barred disk shape and continuously rotates along the Sun-planet axis to align its smallest dimension with the transverse direction of the IMF. **Citation:** Benna, M., et al. (2009), Modeling the response of the induced magnetosphere of Venus to changing IMF direction using MESSENGER and Venus Express observations, *Geophys. Res. Lett.*, *36*, L04109, doi:10.1029/2008GL036718.

1. Introduction

[2] The second flyby of Venus by the MErcury Surface, Space ENvironment, GEochemistry, and Ranging (MESSENGER) spacecraft on 5 June 2007 provided a unique opportunity to further our understanding of the dynamics of the induced magnetospheres surrounding unmagnetized planets in general and that of Venus in particular. The presence of the European Space Agency's Venus Express spacecraft in orbit around the planet at the time of the close passage of MESSENGER allowed both missions to coordinate their observations. This task was made easier by the ideal geometry and timing of the encounter that placed Venus Express far from the planet and able to monitor the undisturbed solar wind while MESSENGER crossed into the inner magnetosphere of Venus. This dual and complementary set of observations illuminated new aspects of the dynamics of the Venus magnetosphere and its interaction with the solar wind.

[3] In this paper, we focus on the temporal evolution of the interplanetary magnetic field (IMF) and its impact on the induced magnetosphere of Venus during the flyby. A magnetohydrodynamic (MHD) model that takes into account the variations of the IMF recorded by Venus Express can account for the magnetic field and ion density profiles measured by MESSENGER and can, ultimately, provide a global view of the state of the Venus magnetosphere at the time of the flyby.

2. Solar Wind Condition at Venus as Observed by Venus Express

[4] From 5 June 22:00 UTC to 6 June 01:00 UTC, the MESSENGER spacecraft traversed the magnetic tail of Venus from dawn to dusk and from north to south reaching its closest approach altitude of 338 km at 23:08 UTC. At the same time, Venus Express was close to its orbital apocenter at a distance of $\sim$11 R_V (where R_V is the radius of Venus), well positioned in the solar wind stream away from the influence of the magnetosphere of Venus. Measurements recorded at that time by the onboard neutral and ion mass spectrometer (ASPERA-4) and magnetometer (VEX-MAG) [*Barabash et al.*, 2007; *Zhang et al.*, 2006] showed that the solar wind velocity was 420 km s^{-1}, its ion density was 8 cm^{-3}, its ion temperature was 10 eV, and the IMF magnitude was 7.5 nT [*Slavin et al.*, 2007]. These values

[1]Solar System Exploration Division, NASA Goddard Space Flight Center, Greenbelt, Maryland, USA.
[2]Johns Hopkins University Applied Physics Laboratory, Laurel, Maryland, USA.
[3]Swedish Institute of Space Physics, Kiruna, Sweden.
[4]Heliophysics Science Division, NASA Goddard Space Flight Center, Greenbelt, Maryland, USA.
[5]Department of Atmospheric, Oceanic and Space Sciences, University of Michigan, Ann Arbor, Michigan, USA.
[6]Department of Terrestrial Magnetism, Carnegie Institution of Washington, Washington, D. C., USA.
[7]Space Research Institute, Austrian Academy of Sciences, Graz, Austria.

0094-8276/09/2008GL036718$05.00

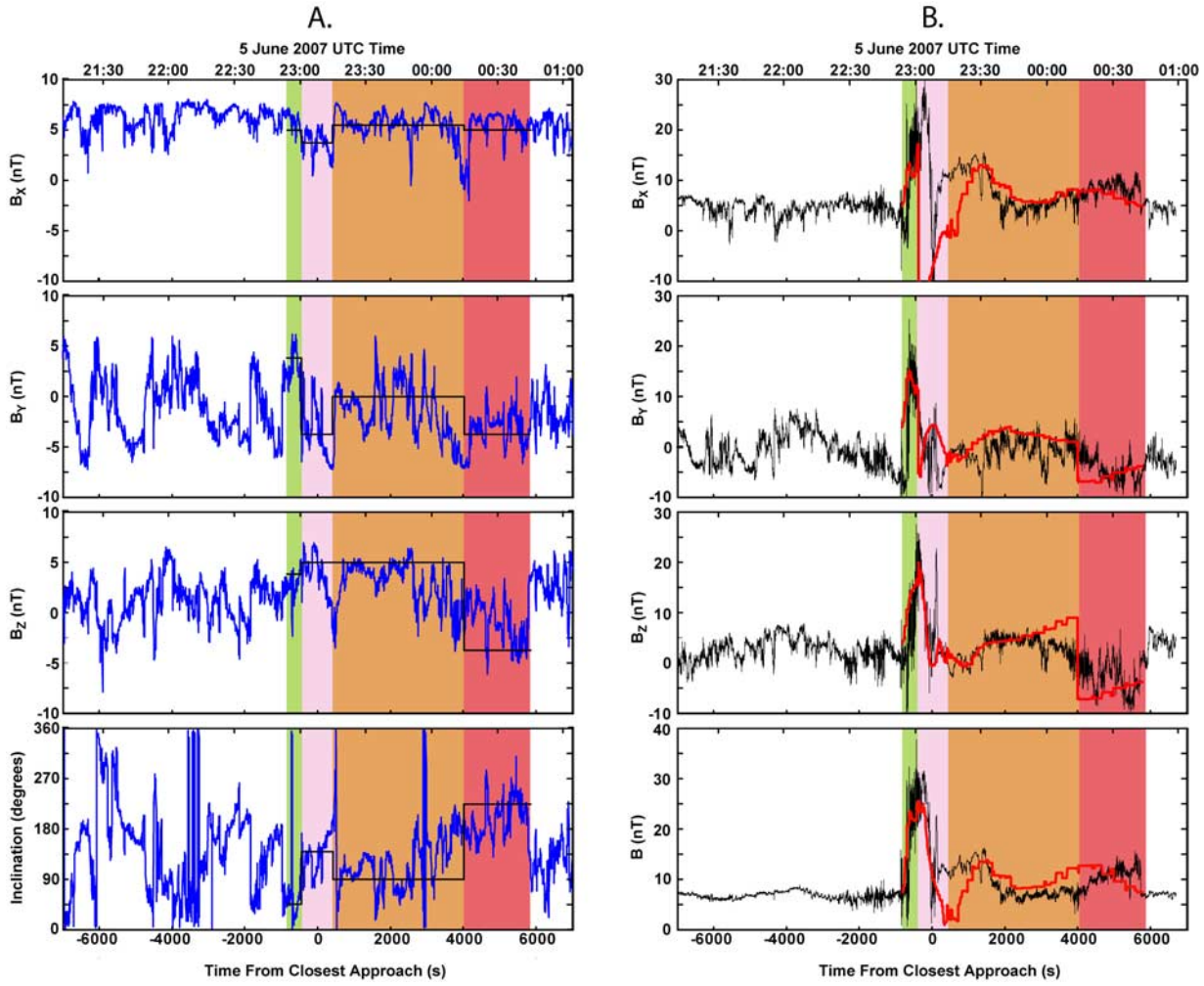

Figure 1. (a) The IMF components and inclination as measured by the VEX-MAG instrument of Venus Express from 5 June 21:00 UTC to 6 June 01:00 UTC (blue lines). The time spent by MESSENGER in the magnetosphere of Venus was subdivided into four temporal segments that correspond to four IMF states. We assume that during each state the IMF did not radically change direction. The temporal extents of these four states are colored (green, pink, orange, and red), and the average magnitude of their components are plotted in black and reported in Table 1. (b) Comparison between the magnetic field measured by the MAG instrument on MESSENGER (black) and the modeled field (red) from 23:55 to 00:45 UTC. The reconstructed magnetic field is the concatenation of the result of the steady-state MHD models computed for the four IMF states.

were relatively stable over the duration of the MESSENGER flyby (with less than 20% fluctuation) and were consistent with a minimum in solar activity [*Meyer-Vernet*, 2007; *Zhang et al.*, 2008]. The IMF vector, however, showed a strong directional variability carried mostly by B_X and B_Y as a rotation in the YZ plane of the Venus Solar Orbital coordinate system (VSO) (in the Venus Solar Orbital coordinate system X is directed from the center of the planet toward the Sun, Z is normal to the Venus orbital plane and positive toward the north celestial pole, and Y is positive in the direction opposite to orbital motion). The variability of the components and the inclination (rotation in the YZ plane) of the IMF over the course of the 4 hours overlapping the flyby (Figure 1a) suggests that the induced magnetosphere of Venus was in a constant transient state during the time of the MESSENGER flyby.

[5] From 22:55 UTC to 00:45 UTC, the period of time during which MESSENGER was confined within the limits of the magnetosphere, the evolution of the IMF can be subdivided into four distinct temporal segments or "IMF states" during which the magnetic field inclination does not drastically change. Table 1 summarizes the temporal extent of these IMF states and their average characteristics.

3. MHD Approach

[6] To simulate the dynamics of the magnetosphere of Venus, one can chose between the two classical approaches usually adopted in MHD numerical modeling: steady-state or time-dependant computations. For this study, neither approach is well suited. The strong variability of the IMF inclination forces the magnetosphere and its layers constantly to reshape themselves to adapt to the new IMF direction, which precludes a simple steady-state MHD solution that uses averaged solar wind parameters and a constant IMF direction. On the other hand, a time-dependent model that

Table 1. Segmentation of IMF Evolution during the MESSENGER Flyby

	Starting Time (UTC)	Ending Time (UTC)	B_X (nT)	B_Y (nT)	B_Z (nT)	Inclination (degrees)
State 1	22:05	23:01	5.0	3.8	3.8	45
State 2	23:01	23:15	3.8	−3.8	5.0	127
State 3	23:15	00:15	5.5	0.0	5.0	90
State 4	00:15	00:45	5.0	−3.8	−3.8	225

correctly tracks changes in the induced magnetosphere over several hours would be computationally intensive (in both run time and memory) and, thus, impractical. We therefore decided to use an intermediary approach that provides a reasonably good representation of the magnetospheric dynamics while remaining computationally practical.

[7] By cross-correlating measurements by the magnetometers on Venus Express and MESSENGER, *Slavin et al.* [2007] showed that the average time needed for the magnetosphere of Venus to adapt to a change in IMF orientation (or transient time constant) is 8.5 min. Because the IMF evolution can be divided into distinct temporal segments having durations comparable to this transient time constant, one can compute a steady-state fluid solution for the IMF state corresponding to each one of these segments. Each steady-state solution will provide magnetic and compositional profiles that are valid only during the corresponding IMF state. By assembling these profiles in their correct temporal order we can reconstruct magnetic and compositional profiles along the entire MESSENGER flyby trajectory.

[8] One should keep in mind that this method is not a substitute for classical time-dependant analysis, but it has the benefit of providing reasonably good information on how the magnetosphere of Venus adapts to abrupt but temporally spaced IMF changes. Concatenation of the compositional and magnetic profiles, however, can introduce artificial discontinuities at the junction between IMF states, which translate to abrupt transitions in the resulting profiles. It is also worth reminding that ideal MHD schemes neglect gyroradius and viscous effects. In the case of Venus, *Pérez-de-Tejada* [1999] showed that viscous forces can play a role in removing a fraction of the solar wind momentum near the terminator.

4. Physical Model

[9] Our model is a variation of the CASIM3D model of *Benna et al.* [2004], which is based on the computational combination of two elements: (a) a magnetohydrodynamic element that solves in three dimensions the MHD equations for ions using an adaptive Total Variation Diminishing Lax-Friedrichs (TVDLF) algorithm, and (b) a chemical element that evaluates the contributions of the source and sink terms within the magnetosphere. The technical details of this model are discussed by *Benna et al.* [2004] and *Benna and Mahaffy* [2006].

[10] In this study, we use a one-fluid, multi-species version of the original algorithm in which H^+ and O^+ densities are tracked separately. To account for the sources of planetary ions within the magnetosphere, a model of a neutral exosphere of Venus was implemented. This exosphere model uses the analytical density profiles of *Rodriguez et al.* [1984], *Mengel et al.* [1989], and *Gunell et al.* [2005] and takes into account the hot and cold components of the hydrogen and oxygen neutrals. The density profiles derived from this model along the Sun-planet and terminator lines are presented in Figure 2.

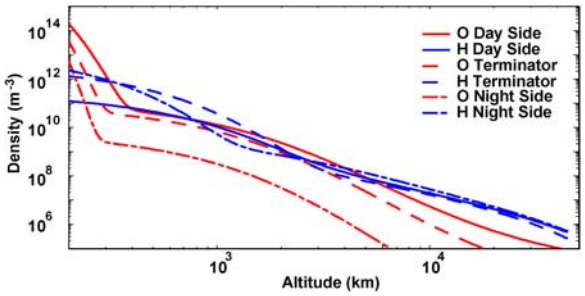

Figure 2. The exospheric density profiles of oxygen (in red) and hydrogen (in blue) for zenith angles of 0° (day side), 90° (terminator), and 180°(night side). These profiles combine the results of *Rodriguez et al.* [1984], *Mengel et al.* [1989], and *Gunell et al.* [2005].

[11] We included only photoionization reactions in our scheme, since it has been shown that impact ionization and charge exchange can be neglected and that photoionization is the main ion production source in the magnetosphere of Venus [*Bauske et al.*, 1998]. The photoionization rates of the exospheric neutrals were assumed equal to those provided by *Kallio et al.* [2006] for minimal solar extreme ultraviolet (EUV) activity. However, because a large fraction of the generated oxygen ions is lost to the ionosphere by finite-gyroradius effects, we artificially reduced the production rate for oxygen by a factor 8 to match the total escape rate of *Kallio et al.* [2006]. Table 2 summarizes the parameters used for this study. The MHD solution for each IMF state was then computed over an adaptive grid with a cell resolution ranging from 300 km near the planet's surface to 9600 km in the undisturbed solar wind.

5. Results

[12] A careful analysis of the four MHD solutions corresponding to each IMF segment confirms that none of the IMF states by itself can fully reproduce the MESSENGER Magnetometer (MAG) observations through the full flyby. These MHD solutions have to be combined in order to understand how the magnetosphere of Venus adapted to successive changes in IMF state. The magnetic field profile along the MESSENGER trajectory that results from the concatenation of these four MHD solutions is presented in Figure 1b. This profile shows good agreement with the

Table 2. Solar Wind Conditions and Parameters Used for This Study

Parameter	Symbol	Value
Solar wind number density	N_{SW}	8 cm^{-3}
Solar wind mean molecular mass	M_{SW}	1 amu
Solar wind speed	V_{SW}	425 km s^{-1}
Solar wind proton temperature	T_{SW}	10 eV
IMF	$\mathbf{B_{SW}}$	see Table 1
Photoionization frequency of H	ν_H	1.39×10^{-7} s^{-1}
Photoionization frequency of O	ν_O	4.55×10^{-7} s^{-1}

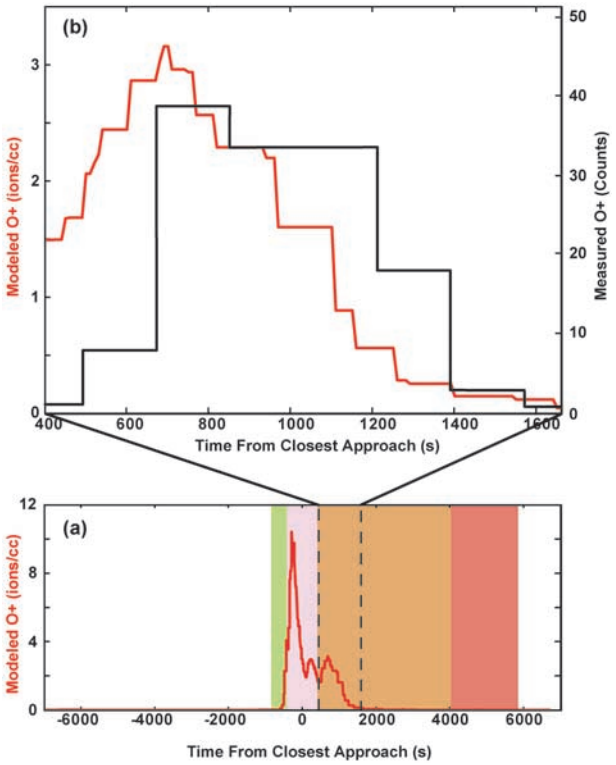

Figure 3. Modeled oxygen ion density along the MESSENGER trajectory: (a) the modeled ion density for the four IMF states; (b) a comparison between the oxygen ion density measured by the EPPS instrument on MESSENGER (black profile in counts/s) and the modeled density (red profile in ions cm^{-3}) from 400 to 1600 s after closest approach.

magnetic field measurements by the MAG instrument, with well-located inbound and outbound bow shock crossings and a magnetic field pile-up within the expected magnitude.

[13] The abrupt sign reversal of B_X and decline of B_Y and B_Z near closest approach is clearly the result of the change of the IMF inclination from 45° to near 140°. The sign change of B_Y and B_Z at 00:15 UTC is also due to a more progressive IMF inclination change from 90° to 230°. The abrupt transitions from one segment to another are mainly due to the fact that we do not consider how fast the IMF changes from one state to another.

[14] The model-derived O^+ pick-up density along the MESSENGER trajectory is shown in Figure 3a. The model predicts three distinct peaks in O^+ density along this trajectory. The first is 330 s before closet approach (CA), the second is 250 s after CA while inside the ionosphere, and the third is at 800 s. Because of other spacecraft observations, the Energetic Particle and Plasma Spectrometer (EPPS) field of view had an unfavorable orientation to detect these O^+ ions until the spacecraft was rotated at ~400 s, so EPPS was unable to confirm the existence of the first two peaks. However, Figure 3b shows that during IMF state 3 there is reasonable agreement between the observed peak in the EPPS counts and the predicted third peak. The first and the third peaks correspond to crossings of the plasma sheet.

[15] This double plasma sheet crossing is the result of the peculiar shape of this boundary. Figure 4 shows the oxygen ion density distribution in the XY and YZ planes. The plasma sheet can be seen as the volume within which these pick-up ions are confined in the magnetotail. The transverse shape of the plasma sheet (as seen in the YZ plane) is a barred disk that constantly rotates around the X-axis to align its smallest dimension with the transverse direction of the IMF. During IMF states 2 and 3, the plasma sheet rotated around the X-axis such that it intersected the MESSENGER trajectory twice, generating two density peaks.

6. Summary

[16] Our semi-time-dependent MHD model is able to reproduce broadly the magnetic and compositional signatures recorded by MESSENGER as responses to IMF changes seen by Venus Express. This model shows that the magnetosphere of Venus fully adapts within a few minutes to changes in IMF inclination (i.e., rotation in the planetary terminator plane). The plasma sheet that confines most of the pick-up ions has an approximately oval shape that continuously rotates around the Sun-planet axis to align its smallest dimension with the transverse direction of the IMF.

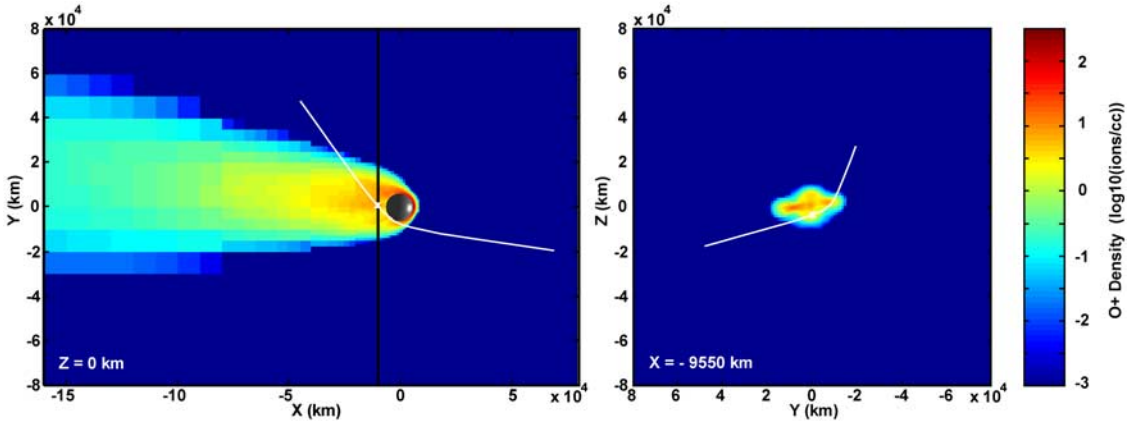

Figure 4. The oxygen ion density distribution in the XY and YZ planes during IMF state 3. The projection of the MESSENGER trajectory onto both planes is depicted in white. The transverse shape of the plasma sheet is a barred disk that allows the spacecraft to cross it at two locations.

The particular orientation of the plasma sheet at the time of the flyby allowed MESSENGER to enter its boundary twice as the spacecraft traveled through the magnetotail.

[17] Fully time-dependant MHD modeling is needed to investigate IMF directional changes that last less than the time needed for the magnetosphere to reconfigure itself. Such models will also be necessary to study the magnetic flux ropes that were seen by MESSENGER in the near-tail region [*Slavin et al.*, 2007].

[18] **Acknowledgments.** This work has been supported by NASA under MESSENGER Participating Scientist grant NNX07AR61G. The MESSENGER project is supported by the NASA Discovery Program under contracts NASW-00002 to the Carnegie Institution of Washington and NAS5-97271 to the Johns Hopkins University Applied Physics Laboratory. Calculations were carried out on the high-performance computing resources of the NASA Center for Computational Sciences. The authors thank the teams of both MESSENGER and Venus Express for making this rendezvous at Venus a success.

References

Bauske, R., A. F. Nagy, T. I. Gombosi, and D. L. Zeeuw (1998), A three-dimensional MHD study of solar wind mass loading processes at Venus: Effects of photoionization, electron impact ionization and charge exchange, *J. Geophys. Res.*, *103*, 23,625–23,638.

Barabash, S., et al. (2007), The Analyser of Space Plasmas and Energetic Atoms (ASPERA-4) for the Venus Express mission, *Planet. Space Sci.*, *55*, 1772–1792.

Benna, M., and P. Mahaffy (2006), Multi-fluid model of comet 1P/Halley, *Planet. Space Sci.*, *55*, 1031–1043.

Benna, M., P. Mahaffy, P. MacNiece, and K. Olson (2004), A multi-scale central difference scheme applied to MHD multi-fluid simulations of cometary atmospheres, *Astrophys. J.*, *617*, 656–666.

Gunell, H., M. Holmström, H. K. Biernat, and N. V. Erkaev (2005), Planetary ENA imaging: Venus and the comparison with Mars, *Planet. Space Sci.*, *53*, 433–441.

Kallio, E., R. Jarvinen, and P. Janhunen (2006), Venus-solar wind interaction: Asymmetries and the escape of O^+ ions, *Planet. Space Sci.*, *54*, 1472–1481.

Mengel, J. G., D. R. Stevens-Rayburn, H. G. Mayr, and I. Harris (1989), Non-linear three dimensional spectral model of the Venusian thermosphere with super-rotation: II. Temperature, composition and winds, *Planet. Space Sci.*, *37*, 707–722.

Meyer-Vernet, N. (2007), *Basics of the Solar Wind*, 478 pp., Cambridge Univ. Press, New York.

Pérez-de-Tejada, H. (1999), Viscous forces in velocity boundary layers around planetary ionospheres, *Astrophys. J.*, *525*, L65–L68.

Rodriguez, J. M., M. J. Prather, and M. B. McElroy (1984), Hydrogen on Venus: Exospheric distribution and escape, *Planet. Space Sci.*, *32*, 1235–1255.

Slavin, J. A., et al. (2007), MESSENGER and Venus Express observations of the solar wind interaction with Venus: A dual spacecraft study, *Eos Trans. AGU*, *88*(52), Fall Meet. Suppl., Abstract P41B-06.

Zhang, T. L., et al. (2006), Magnetic field investigation of the Venus plasma environment: Expected new results from Venus Express, *Planet. Space Sci.*, *54*, 1336–1343.

Zhang, T. L., et al. (2008), Initial Venus Express magnetic field observation of the magnetic barrier at solar wind minimum, *Planet. Space Sci.*, *56*, 790–795.

M. H. Acuña and M. Benna, Solar System Exploration Division, NASA Goddard Space Flight Center, 8800 Greenbelt Road, Greenbelt, MD 20771, USA. (mehdi.benna@nasa.gov)

B. J. Anderson, R. E. Gold, G. C. Ho, S. M. Krimigis, H. Korth, and R. L. McNutt Jr., Johns Hopkins University Applied Physics Laboratory, 11100 Johns Hopkins Road, Laurel, MD 20723, USA.

S. Barabash, Swedish Institute of Space Physics, Box 812, SE-981 28 Kiruna, Sweden.

S. A. Boardsen, M. Sarantos, and J. A. Slavin, Heliophysics Science Division, NASA Goddard Space Flight Center, 8800 Greenbelt Road, Greenbelt, MD 20771, USA.

G. Gloeckler, J. M. Raines, and T. H. Zurbuchen, Department of Atmospheric, Oceanic and Space Sciences, University of Michigan, 2455 Hayword Street, Ann Arbor, MI 48109, USA.

S. C. Solomon, Department of Terrestrial Magnetism, Carnegie Institution of Washington, 5241 Broad Branch Road, NW, Washington, DC 20015, USA.

T. L. Zhang, Space Research Institute, Austrian Academy of Sciences, Schmiedlstrasse 6, A-8042 Graz, Austria.